Geomechanics and Engineering, *Vol. 38, No. 1 (2024) 79-91*
https://doi.org/10.12989/gae.2024.38.1.079

Model tests on the bearing capacity of pervious concrete piles in silt and sand

Han Xia[1,2a], Guangyin Du*[1,2], Jun Cai[1,2,3b] and Changshen Sun[1,2c]

[1]*School of Transportation, Southeast University, Jiulong Lake Campus, China*
[2]*National Demonstration Center for Experimental Road and Traffic Engineering Education (Southeast University), China*
[3]*Changjiang Institute of Geotechnique and Survey, MWR, China*

(*Received February 1, 2022, Revised June 17, 2024, Accepted July 2, 2024*)

Abstract. The settlement, bearing capacity, axial force, and skin friction responses of pervious and impervious concrete piles in silty and sandy underlying layer foundations and of pervious concrete piles in model tests were determined. The results showed that pervious concrete piles can exhibit high strengths, provide drainage paths and thus reduce foundation consolidation time. Increasing the soil layer thickness and pile length could eliminate the bearing capacity difference of pervious piles in a foundation with a silty underlying layer. The pervious concrete piles in the sandy underlying layer were more efficacious than those in the silty underlying layer because the sandy underlying layer can provide more bearing capacity than the silty underlying layer. The results indicated that the performances of the pervious concrete piles in the sand and silt foundations differed. The pervious concrete piles functioned as floating piles in the underlying layer with a lower bearing capacity and as end-bearing piles in the underlying layer with a higher bearing capacity.

Keywords: bearing characteristics; model test; pervious concrete piles; sand foundation; silt foundation

1. Introduction

The construction of embankments with deep weak soils is a widespread challenge and risk. In general, weak ground needs to reach the desired settlement or shear strength before infrastructure construction (Qin 2020). To reinforce soft soil foundations, many methods have been used under different conditions (Le 2022, Wang 2022, Peng, 2022). Rubber drainage columns can reduce liquefaction more effectively than can gravel drainage columns (Bahadori 2018), but the drainage consolidation method may be a time-consuming conventional method. It is difficult for PHC (prestressed high-strength concrete) pile design to guarantee the quality of pile joints and be economical, and the construction of this pile type could greatly disturb the surrounding soil. Deep mixing columns can reduce the seismic response of foundations (Hasheminezhad 2019), yet it is difficult to control the quality of banks in the bottom part of deep foundations (Hasheminezhad 2020, Pan 2020). Since the middle of the last century, many countries have studied the application of pervious concrete. The most representative pervious concrete is sand-free concrete, which was first proposed by Tamai (1992), and it has been used for water purification. With the properties of a high pore ratio and high permeability, scholars have focused on pervious concrete because it has not only a high permeability but also a high strength and stiffness (Neville, 1996, Montes 2005, Haselbach 2007, Kayhanian 2012).

Pervious concrete is a mixture of narrowly graded coarse aggregates and cement that forms an interconnected macroporous internal matrix and a very porous structure (Neithalath 2010, Huang 2010, ACI 2010, Yahia 2014). The porosity of pervious concrete usually ranges from 15% to 35% (ACI. 2006), its compressive strength is between 2.8 and 28.0 MPa (Malaiskiene 2020, Teja Munaga 2020), and its permeability coefficient is usually 2.0-5.4 mm/s (Tennis 2004). Pavement materials are used for the subsequent application and support of pervious concrete (Ghafoori 1995, Tennis 2004 Qin 2016); they improve the environmental conditions for the application of pervious concrete to pavement (Schaefer 2006).

Suleiman (2014) proposed a new ground improvement method of pervious concrete piles. Compared with other piles, pervious concrete piles can provide a good drainage system and have a high shear strength. During the consolidation process, the water in the soil seeps through the pervious concrete in the radial direction, and the water drains from the core hole of the pile in the vertical direction. Additionally, pervious concrete can provide a rigid surface and a high friction resistance, promoting its application. Because of the use of a higher-strength cement, pervious concrete piles have more bearing capacity than sand drainage columns. Based on these advantages, pervious concrete piles have attracted the attention of scholars. Lin (2016) demonstrated the load–displacement response, load transfer, and load bearing capacity of pervious concrete piles under compressive loading; Cui (2021) revealed the corresponding mechanism of porosity reduction and

*Corresponding author, Professor
E-mail: guangyin@seu.edu.cn
[a]Ph.D.
E-mail: evansha@126.com
[b]Ph.D.
E-mail: caijun129@seu.edu.cn
[c]Master's Degree
E-mail: 220162679@seu.edu.cn

ISSN: 2005-307X (Print), 2092-6219 (Online)

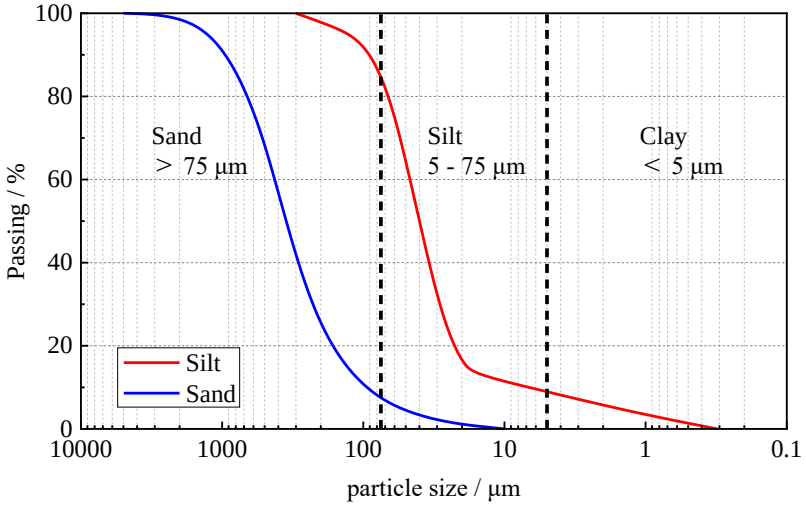

Fig. 1 Grain size distribution of the silty soil

Table 1 Parameters of the soils

Soil	w_L (%)	w_P (%)	I_P	ρ_n (g/cm^3)	ρ_{dmax} (g/cm^3)	G_s (g/cm^3)	c (kPa)	φ (°)	E_s (MPa)
Silt	32.8	24.4	8.4	1.79	-	2.74	28.5	23.9	8.48
Sand	-	-	-	-	1.429	2.66	3.5	32.6	24.81

proposed a dynamic clogging model; Ni (2016) proposed a stress response trend. Compared with conventional piles, pervious concrete piles can accelerate the load response and pore water dissipation (Zhang *et al.* 2017) and provide a higher ultimate shear strength (Rashma *et al.* 2021). These results show that this type of pile has the advantages of both permeability and strength and can be combined with soil to reform a composite foundation.

The underlying layer of a foundation is essential for foundation stability; if the capacity of the underlying layer is less than that of the composite foundation, the bearing capacity must be checked. Pervious concrete piles have been found to be sensitive to the type of underlying layer in a composite foundation: for example, a sand layer (Bahadori 2015, Bahadori 2018) can provide more bearing capacity than a silt layer. On the one hand, the pervious concrete pile has high strength and can provide a vertical bearing force; on the other hand, the rough surface of the pile can provide a large frictional force. To reveal the mechanical performance and bearing characteristics of pervious concrete piles in different underlying layers, a model test method was used to evaluate the mechanical response of pervious concrete piles in sandy and silty underlying layers.

2. Test materials

2.1 Soils and engineering properties

The silty soil was taken from the Dafenggang section of the Huaiyan expressway, Yancheng city. This area hosts a set of coastal loose deposits that formed during the Miocene to middle Pleistocene and is mainly composed of fine-grained clay and silty clay. The middle part is mainly composed of coarse-grained sand layers, and the upper part is mainly composed of silty clay. The sandy soil was taken from the Nanjing section of the Yangtze River. In this area, the upper soil consists of silty clay, fine sand, and silt, which formed Holocene alluvial deposits.

To analyze the engineering properties of the silt and sand, laboratory tests were conducted. Fig. 1 shows the grain size distributions of the silt and sand. The sand sample is fine sand, with a sand particle content of 92.7% and silt particle content of 7.3%. The silt includes 14.5% sand particles and 8.7% of silt particles. The engineering properties are shown in Table 1.

2.2 Pervious concrete

According to previous research, pervious concrete consists of only cement and aggregate. Therefore, following the suggestions of the Technical Specifications for Pervious Concrete Pavements (CJJ/T 135-2009), 3-5 mm aggregates and P.O. 52.5 cement (ordinary Portland cement) were used, and the cement and aggregate parameters are shown in Tables 2 and 3.

A series of tests were carried out to reveal the relationship between the designed porosity and effective porosity. The analysis considered the standard deviation and average values. As shown in Fig. 2(a), as the designed porosity increases, the effective porosity also increases. The designed porosities of 30% and 35% have the most similar average effective porosities. Thus, 30% and 35% designed porosities were selected for further analysis. The relationships among the 28-day compressive strength,

Table 2 The parameters of the aggregates

Aggregate size (mm)	Specific gravity G_s (g/cm^3)	Density ρ (g/cm^3)	porosity (%)
3-5	2.632	1.587	39.7

Table 3 The parameters of the cement

Compressive strength (MPa)		Setting time (min)		Specific surface (m^2/kg)
3 days	28 days	Initial setting	Final setting	
33.8	58.0	115	184	381

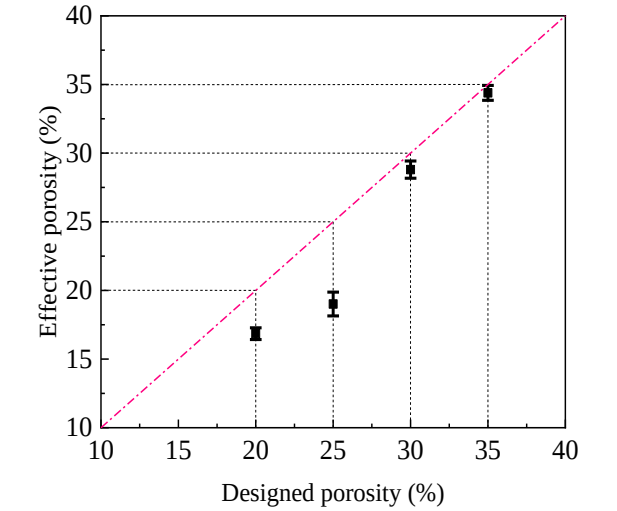

Fig. 2 Relationship between the designed porosity and effective porosity and between the compressive strength and permeability

designed porosity, and permeability are shown in Fig. 2(b). The 28-day compressive strength decreased with the designed porosity, but the permeability increased with the designed porosity. There is an inversely proportional relationship between the 28-day compressive strength and permeability. Therefore, considering the permeability and strength of pervious concrete, 30% porosity was selected as the target porosity.

Table 4 Mix proportions per cubic meter of the pervious concrete

Target porosity (%)	Aggregate (kg/m^3)	Cement (kg/m^3)	Water (kg)
30	1.555	261	78

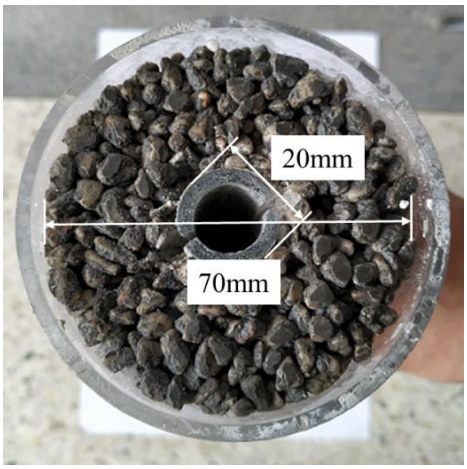

(a) Top view

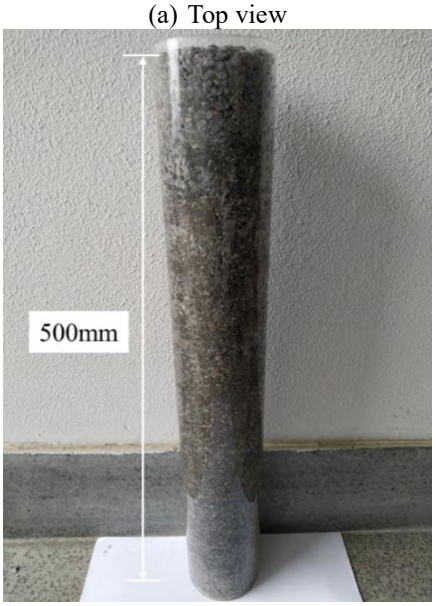

(b) Side view

Fig. 3 Model pile

According to Technical specification for pervious cement concrete pavement (CJJ/T 135-2009), the mix proportions of the pervious concrete per unit volume were obtained, as shown in Table 4.

2.3 Model pile

The technical code for the composite foundation of a pervious pile (DB37/T 5124-2018) recommends that the diameter and pile spacing for the composite foundation of the pervious pile be 300-500 mm, and Zhang *et al.* (2017) suggested that the pile spacing be three times the pile diameter. Therefore, the external diameter of the model was 70 mm (D), the internal diameter was 20 mm (d), and the length was 500 mm (l) (Fig. 3).

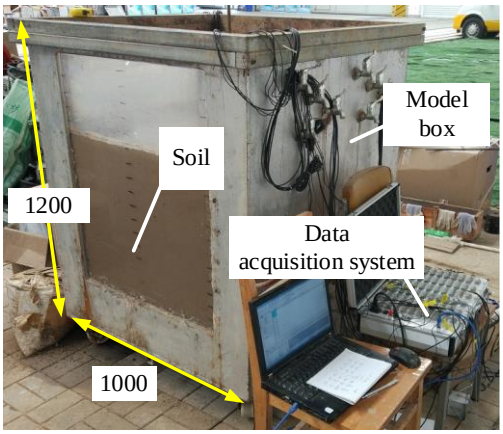

(a) Test facility

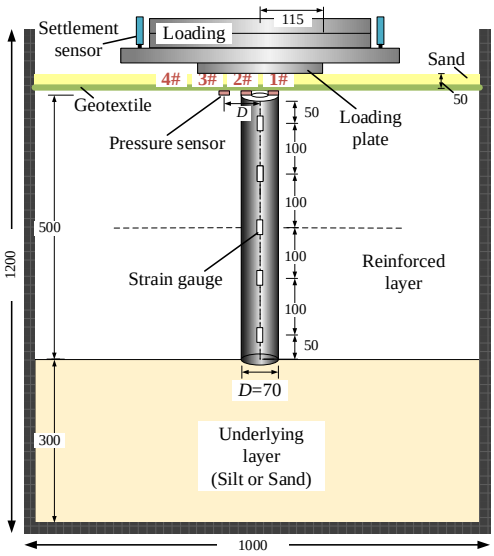

(b) Sensor arrangement

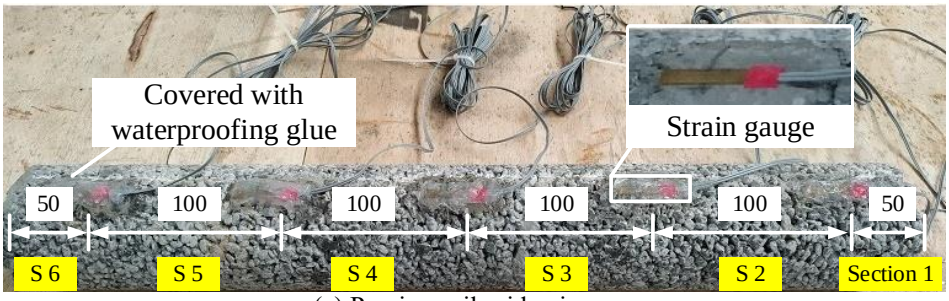

(c) Pervious pile side view

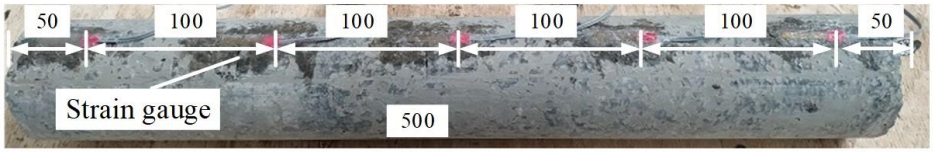

(d) Impervious pile side view

Fig. 4 Test facility (unit: mm)

3. Test facility and processes

3.1 Test facility

To avoid boundary effects, the size of the model box was chosen to be 1 m × 1 m × 1.2 m, and the acquisition system is shown in Fig. 4(a). Before the test, the pervious concrete piles were cured for 28 days under standard conditions. Then, the pile was divided into six sections, each 100 mm long, except for the top and the end sections of the pile, which were only 50 mm long each. Pressure sensors were used to measure stress, and strain gauges were used to measure strain (see Fig. 4(b)-4(d)). The model box was filled with soil, and the underlying layer was either silty or sandy soil.

Eight layers (10 cm each) were used to fill the soil in the model box to maintain soil uniformity. When filling the sand soil, the water for each layer was added first before the sand, which was then compacted to the specified elevation.

Table 5 Parameters for the soil in the test

Soil	ρ (g/cm^3)	w (%)	e	D_r	S_r (%)
Silt	1.919	29.5	0.849	2.74	95.2
Sand	1.968	23.8	0.673	2.66	94.1

When a reasonable depth was reached, the model pile was placed, and filling continued to the designed height. For the silty soil, the silt was dried and crushed; then, the silty soil with a water content of 30% was thoroughly mixed to achieve good uniformity, reducing the air bubbles in the soil. After filling, each layer was allowed to rest for 12 hours, and the model box was covered with plastic film to prevent evaporation. When filling to a height of 80 cm, the pile was driven to the designed depth. Afterward, the model box was allowed to rest for at least seven days, until the excess pore pressure dissipated completely. Then, the soil was sampled and tested; the average values of the parameters are shown in Table 5.

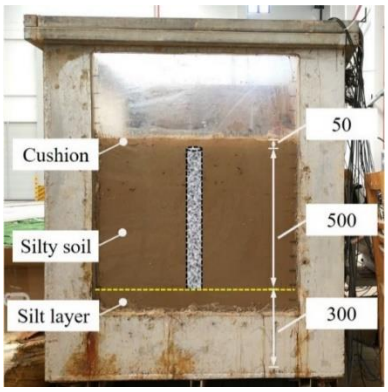

(a) Underlying layer: silty soil

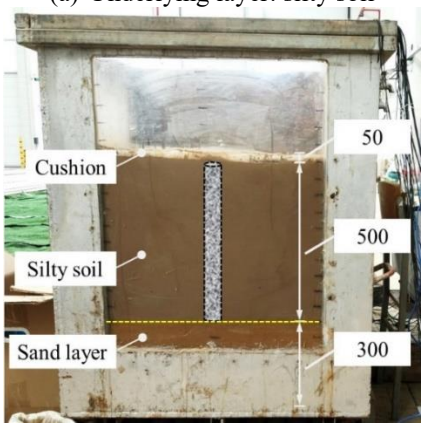

(b) Underlying layer: sandy soil

Fig. 5 Pervious concrete piles with different underlying layers (unit: mm)

3.2 Test processes

Coarse sand with a geotextile is placed on the foundation as the cushion, with a thickness of 50 mm (Fig. 5). According to the Chinese Technical Code GB/T 50783-2012 for composite foundations, the slow continuous loading method was applied as the loading procedure. First, 5%-10% of the maximum load was used for preloading; afterward, the cargo was unloaded, and the formal test started. When the settlement slowed and stabilized during the trial, the next load stage continued. Due to the higher bearing capacity of the sand foundation, the loads applied at each step were twice those of the silt foundation. The loading termination criterion was the observation of a crack on the surface of the composite foundation, and the maximum loads for the silt and sand foundations were 4800 N and 6800 N, respectively. The drainage pipe was set to acquire the bearing characteristics when draining the soil water, and the maximum pumping rate was 100 ml/min.

4. Comparison of the test results for the pervious and conventional piles

4.1 Axial force

A comparison of the axial forces in the silt between the pervious and impervious pile cases under load levels of

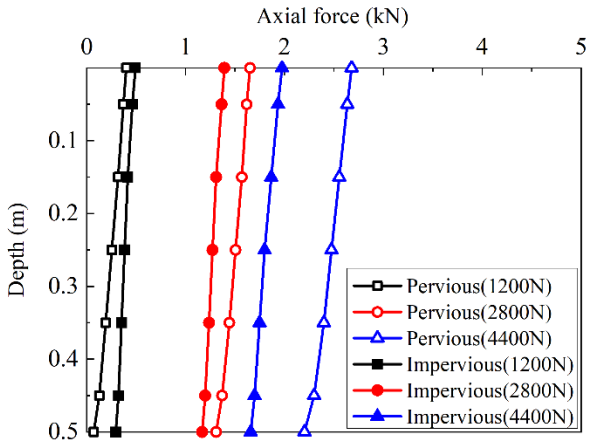

Fig. 6 The axial force results obtained under different loads

1200 N, 2800 N, and 4400 N is shown in Fig. 6. The results show that at low load levels, there is little difference in the axial forces at the tops of the pervious and impervious piles. This indicates that in the initial loading stage, the loads shared by the piles in the composite foundation are similar. However, the amplitude of the axial force attenuation of pervious piles along the depth direction of the foundation is greater than that of impervious piles, indicating that for pervious piles, the lateral friction resistance along the pile body is greater than that for impervious piles. As the load increases, the increase in axial force at the top of the pervious pile is smaller than that at the top of the impervious pile. This is because pervious piles are permeable, and the bearing capacity of the soil around the pile increases rapidly under drainage and consolidation. The foundation soil bears a greater load, and the pile bears a lesser load, resulting in a smaller increase in the axial force on the pile. In the later stage of loading, both the pervious and impervious piles experienced varying degrees of penetration into the underlying layer. Due to the high lateral friction resistance of pervious piles and the high bearing capacity of the foundation soil, the penetration of these pile into the underlying layer is relatively small, and the piles bears more of the loads (Liu 2012, Yu 2020), resulting in higher axial forces.

4.2 Pore water pressure dissipation

The curves of the pore water pressure dissipation results in the middle of the pervious and impervious concrete piles during pile sinking are shown in Fig. 7. During the penetration of a pervious concrete pile into the foundation, significant excess pore pressure is generated mainly at the middle of the pile body (d = 250 mm, depth), which is 1D (D =50 mm, diameter) away from the center of the pile, while the impact of excess pore pressure at position 2D (100 mm) is significantly smaller. The green horizontal line in Fig. 7 represents the 1 kPa overpressure line. For position *1D*, the overpressure drops below 1 kPa at approximately 500 seconds. The dissipation time of the excess pore pressure of the pervious piles at position 1D is approximately 75% shorter than that of the impervious piles

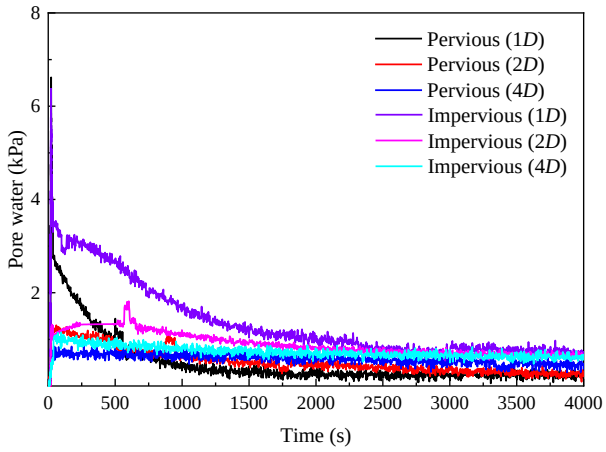

Fig. 7 The excess pore water pressure dissipation

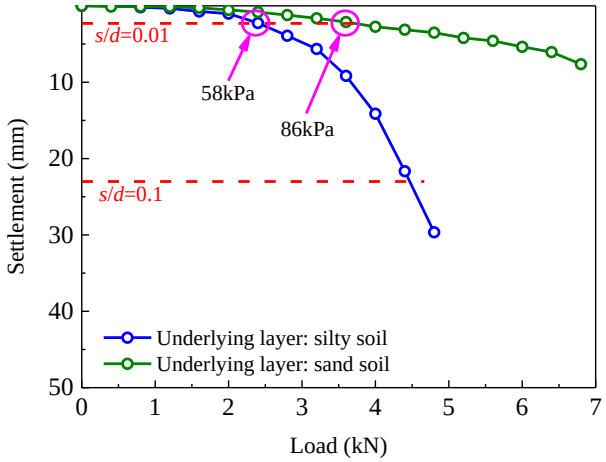

Fig. 8 Load–settlement responses of foundations with different underlying layers

at the same position, while the dissipation time of the excess pore pressure of the pervious piles at position 2*D* is approximately 50% shorter than that of the impervious piles. These results are consistent with those of former researchers (Wang 2024, Gong 2022). Therefore, the dissipation rate of excess pore pressure in pervious concrete piles is significantly faster than that in impervious concrete piles. In the radial direction, the excess pore water pressure dissipation is positively correlated with distance, which may be related to the longer soil drainage path and greater compactness of the foundation.

5. Comparison of the results obtained for the sandy and silty underlying layers

5.1 Load–settlement response

The bearing capacity of a composite foundation with a sandy underlying layer may be very high, and it is difficult for this material to reach its ultimate bearing capacity state during model test loading. According to the Technical Code for Composite Foundation (GB/T 50783-2012), a test can be terminated when the load reaches the predetermined maximum value. Fig. 8 presents the measured load–settlement responses of the different underlying layers. With increasing load, the settlement of the silt foundation increases in a stepwise manner. The characteristic value of the bearing capacity of the foundation with a sandy underlying layer can reach 86 kPa. The foundation with a silty underlying layer is 58 kPa; the difference in the bearing capacity between these two foundations is 28 kPa. The bearing capacity of the silt foundation is 33% lower than that of the sand foundation. However, with increasing soil layer thickness and pile length, soil can provide more support and thus increase the bearing capacity of the foundation (Zhou *et al.* 2015). As a result, the difference in bearing capacity of pervious concrete piles in different underlying layers may decrease.

Fig. 9 shows the pile–soil stress ratio for foundations with different underlying layers. Compared with that of the silty underlying layer, the pile–soil stress ratio of the sandy

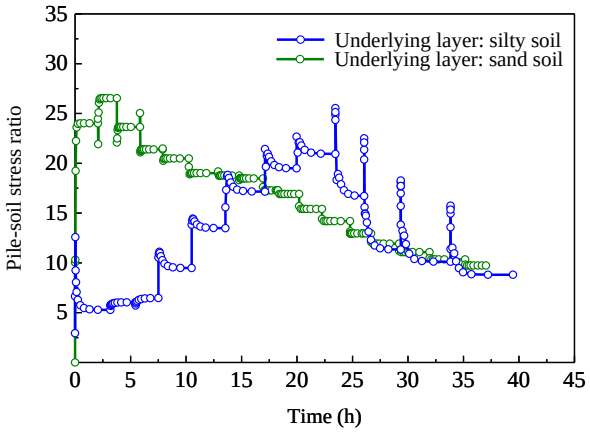

Fig. 9 Pile–soil stress ratios for foundations with different underlying layers

underlying layer shows a rapid change with time throughout the loading process. The maximum values of the pile–soil stress ratio of the pervious piles in the silty and sandy underlying layers reach 26 and 27, respectively. These results indicate that although the two curve types are different, the final pile–soil stress ratio is almost the same. This is because the pile tip is in the underlying layer, and the deformation of the pile is small. The load is mainly transmitted to the bearing layer through the pile, while the load shared with the foundation soil is negligible. Therefore, foundation soil consolidation and bearing capacity improvement have little impact on the pile–soil stress ratio. The dissipation of pore water can increase during consolidation of the sand underlying layer. As a result, the drainage path in the sandy underlying layer is shorter than that in the silty underlying layer, the consolidation is more efficient, and the pile–soil stress ratio is more easily stabilized. Therefore, throughout the loading process, the change in the pile–soil stress ratio of the pervious pile in the underlying sandy soil layer is nearly zero at each load level, and the change in the pile–soil stress ratio is small in the later stage of loading.

The variations in the pile–soil stress ratios (final value) with the load in the silty and sandy underlying layer

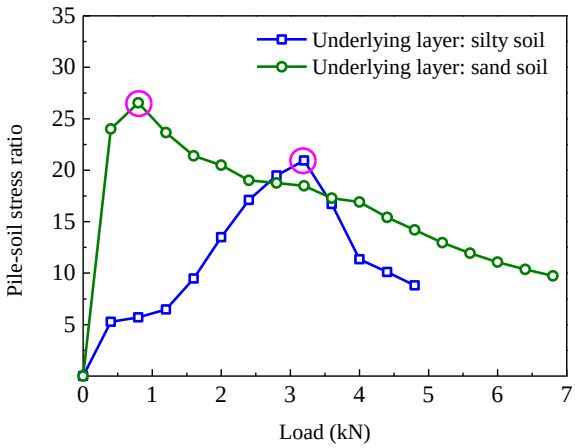

Fig. 10 Changes in the pile–soil stress ratios with increasing load

foundations is shown in Fig. 10. When the load is low and the underlying layer is the bearing layer, the bearing capacity of the pervious concrete pile is high, and the settlement of the composite foundation under the load is small. In this case, the pile bears more of the stress, and the pile–soil stress ratio is approximately 24, while the pile–soil stress ratio of the foundation in the underlying silty soil layer is only approximately 5. With increasing load, the pile–soil stress ratio increases, reaching a maximum value of 27. The pile–soil stress ratio of the pervious concrete pile composite foundation with a silty underlying layer is 6. After the pile–soil stress ratio of the sandy underlying layer peaks, it decreases gradually. The pile–soil stress ratio of the underlying silty layer increases to 21 and then decreases. Due to the small settlement and side friction of pervious concrete piles, the load transfer along the foundation depth is efficient. With increasing load, the pile tip penetrates the underlying layer, the bearing capacity of the foundation soil increases rapidly during this process, the shared load increases, and the pile–soil stress ratio decreases gradually.

The results of the pile–soil stress ratio show that the pile–soil stress ratio of the pervious pile foundation is only high in the early stage. With increasing load, the difference between the pile–soil stress ratios of the two underlying layers before the penetration of the underlying layer is low. Their bearing characteristics are also similar, as discussed below.

5.2 Bearing characteristics

The strain distribution of a pile can be obtained with strain gauges along the shaft of the pile, and the average pile axial force at the measured depth (Q_Z) in the model pervious concrete pile can be calculated as

$$Q_z = E\varepsilon A \tag{1}$$

where E is the elastic modulus of the pile with a porosity of 30%, GPa; ε is the strain of the pile at the designed section; and A is the cross-sectional area of the pile, m^2.

The axial force distribution between different underlying layers is shown in Fig. 11. The figure shows the

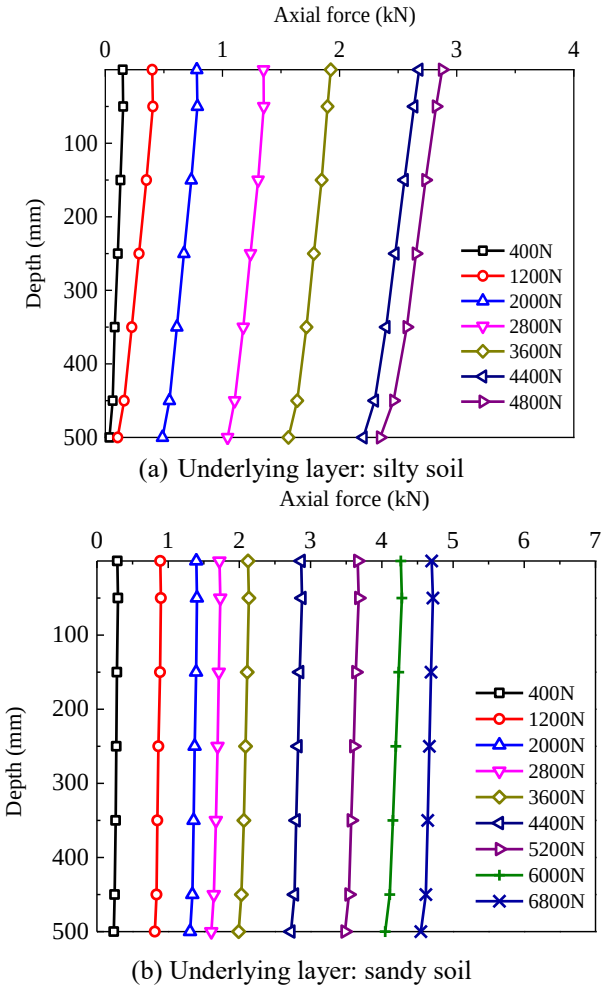

Fig. 11 Distribution of the axial force between different underlying layers

difference in axial force characteristics between the silty and sandy underlying layers. The axial force of the pervious concrete pile decreases with increasing depth in the foundation with a silty underlying layer. The axial force in the sand foundation is uniformly distributed with depth, except at the pile tip. The pile can provide more bearing capacity with the underlying layer of sandy soil than with the underlying layer of silty soil. Therefore, the axial force at the pile top is more significant. The maximum axial force in the sand can reach 4.7 kN and 1.8 kN greater than the maximum axial force in the silt.

The responses of the axial force under different loads of the underlying layers are plotted in Fig. 12. The axial force of the pervious concrete pile in the sandy underlying layer is greater than that in the underlying silty layer under various loads. Under a lower load, the settlement deformation of the composite foundation with a silty underlying layer is obvious, so the skin friction is considerable, and the attenuation of the axial force along the depth is more prominent. With increasing load (under 2800 N and 4400 N), the difference between the axial force of the pervious pile in the silty underlying layer and that in the sandy underlying layer decreases gradually. This phenomenon indicates that the load shared by the pile

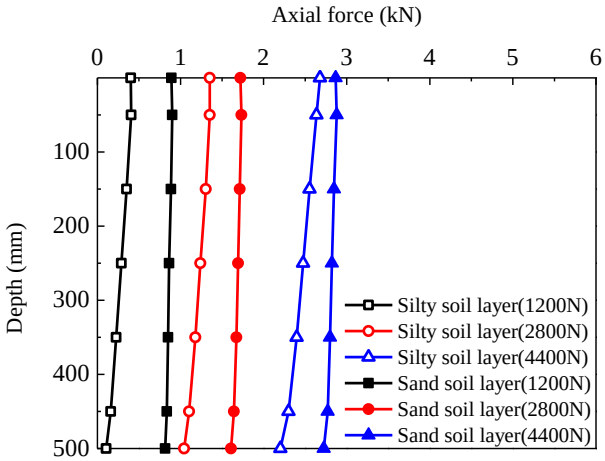

Fig. 12 Comparison of axial forces under different loads

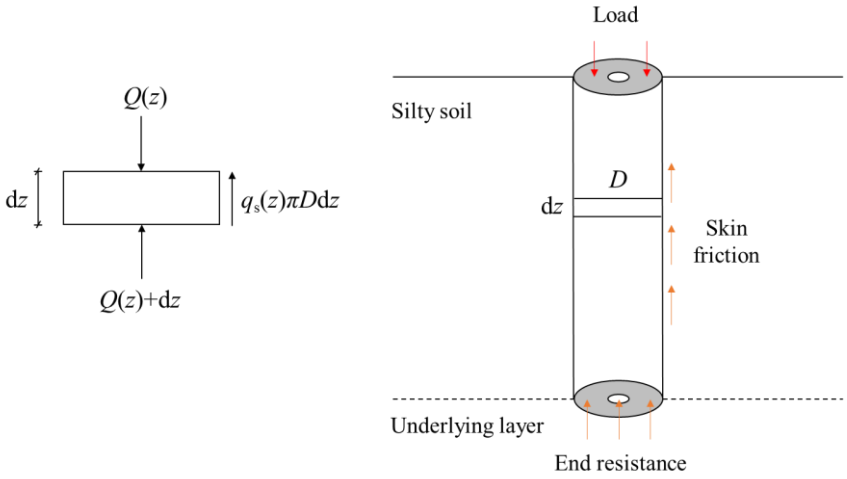

Fig. 13 Notations for equations of equilibrium

increased significantly. At the same time, the axial force attenuation of the porous concrete pile in the silty underlying layer is more evident along the depth direction, so its side friction resistance is more remarkable. The greater the resistance at the pile end, the more external load it bears. The pile experiences significant downward penetration deformation, which leads to an increase in the additional stress in the underlying soil layer and a decrease in the load born by the reinforced soil layer (Han 2023).

The skin friction of a pile foundation is an essential parameter for its design and analysis (Wu et al. 2015). The distribution of the skin friction along the shaft of a pile can be computed by dividing the difference between two consecutive axial forces by the surface area between the two strain gauges.

An element pile mass with side measurements of dz and D is shown in Fig. 13. According to the equations of equilibrium, the skin friction q_s is

$$q_s(z) = -\frac{1}{\pi D} \cdot \frac{\mathrm{d}Q(z)}{\mathrm{d}z} \tag{2}$$

where z is the depth, mm; N is the axial force, kN; and D is the diameter of the pile, m. The skin friction (Q_s) of pervious concrete is related to the displacement of the pile and soil.

If the length of the pervious concrete pile is l (mm), the whole skin friction Q_s is

$$Q_s = -\frac{1}{\pi D}\int_0^l \frac{\mathrm{d}Q(z)}{\mathrm{d}z} = -\frac{Q}{\pi dl} \tag{3}$$

Then, the pile skin friction in each section can be calculated with

$$q_s = \frac{Q_1 - Q_2}{\pi D \Delta L} \tag{4}$$

where Q_1 and Q_2 are the axial forces of the two adjacent cross-sections, kN, and ΔL is the length between the two cross-sections.

Fig. 14 presents the distributions of unit skin friction along the pile shaft in different underlying layers. The results show that the unit skin friction generally increases with the applied load. In Fig. 14(a), the pile skin friction is mainly concentrated at the pile tip. Because the pile top penetrates the cushion layer, the pile top skin friction is negative at the initial stage of loading in both the silty and

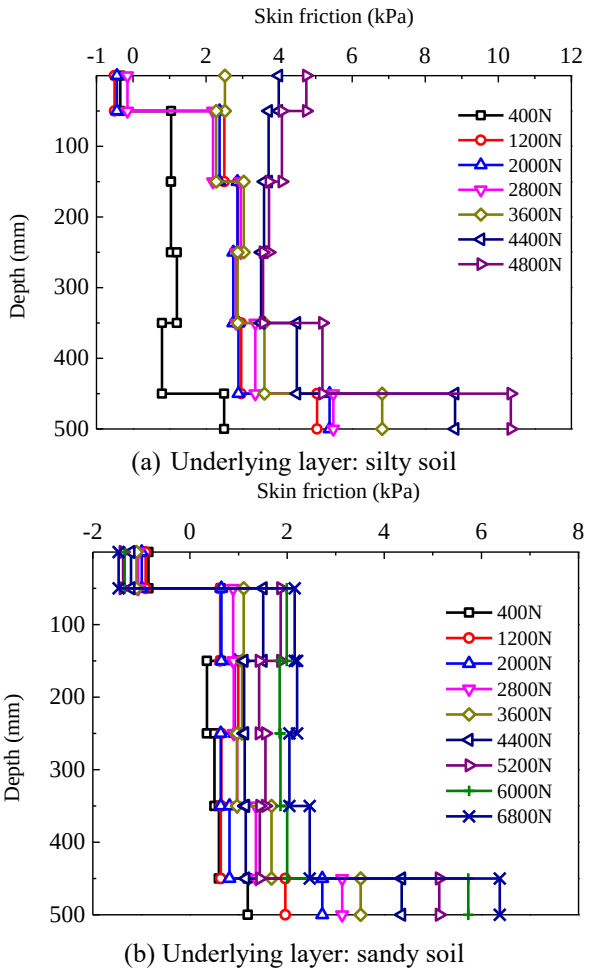

(a) Underlying layer: silty soil

(b) Underlying layer: sandy soil

Fig. 14 Comparison of skin frictions under different loads

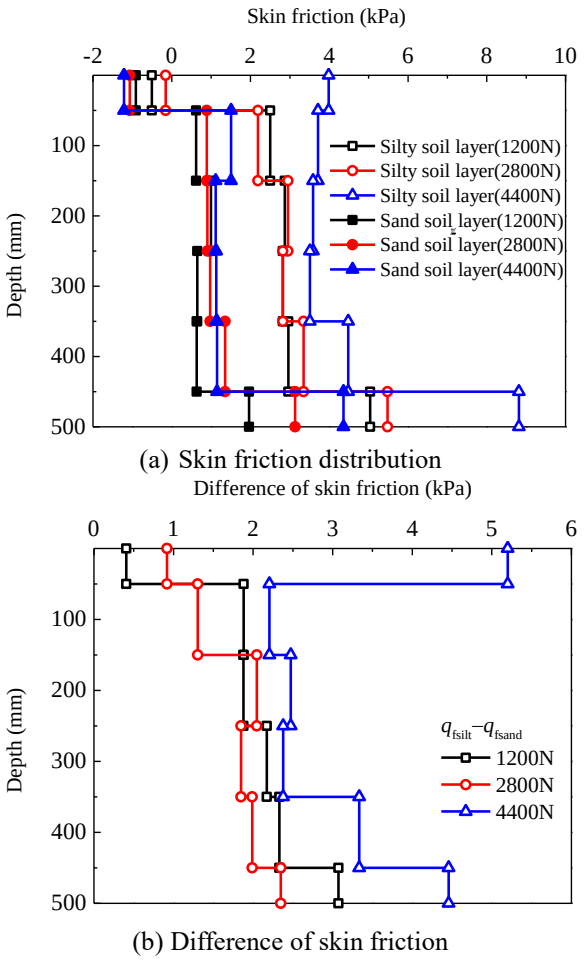

(a) Skin friction distribution

(b) Difference of skin friction

Fig. 15 Comparison of skin friction results along pile depth

sandy underlying layer foundations. Comparing Fig. 14(a) and Fig. 14(b), the pile settlement in the silty underlying layer foundation is more significant, and its skin friction resistance is also better. Therefore, the pile side friction resistance difference in the whole process is positive.

A comparison of the skin friction characteristics of the silty and sandy underlying layer foundations during loading is shown in Fig. 15. In Fig. 15(a), the skin friction is mainly concentrated at the pile tip (sections 5 and 6), and the skin friction of the pile top is negative at the initial stage of loading (400-2800 N in section 1). Fig. 15(b) shows that the skin friction of the pile in the silty underlying layer is more efficient than that in the sand layer during the consolidation process because the settlement of the underlying layer of silt is more evident than that of the sand layer. Therefore, the difference in the pile skin friction is positive during the loading process. The contrast of the pile skin friction increases with depth in both the silt and the underlying layer, so increasing the pile length can significantly increase the bearing capacity of the pile with a small tip resistance. Under a load of 4400 N, the difference in the pile skin friction under the two bearing modes also increases gradually along the depth direction except for at the pile top (0–50 mm). Therefore, increasing the pile length can significantly increase the bearing capacity of the pile.

The relationship between the pile skin friction and the settlement of the composite foundations with silty and sandy underlying layers is shown in Fig. 16. The results show that the skin friction of section 6 (pile tip) is considerably greater than that of the other sections (sections 1–5). In the early settlement stage, the pile skin friction is also more significant than that at different positions. There are two reasons for this phenomenon. One reason is that the underlying layer is compacted by pile sinking, the soil in the pile tip is denser than that in other places; the other reason is that the increase in skin friction with the small settlement is still primarily due to the soil plugging effect. The skin friction of other parts of the pile increases slightly because the relative settlement of the pile and soil is small (Yang, 2015). Considering the settlement of the composite foundation in the last loading process (see Fig. 8), the minor increase in skin friction, and the significant compensation, this case indicated that the deformation of the composite foundation might be caused by the adjustment deformation of the cushion when the pile top pierces upward into the pillow.

Fig. 17 shows a comparison of the mean skin frictions of the pervious concrete piles under the different loading processes. The results indicate that the skin friction of the pervious pile increases slowly in the sandy underlying

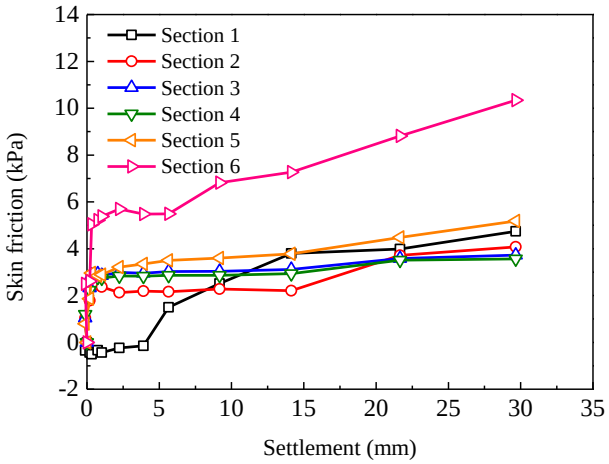

(a) Underlying layer: silty soil

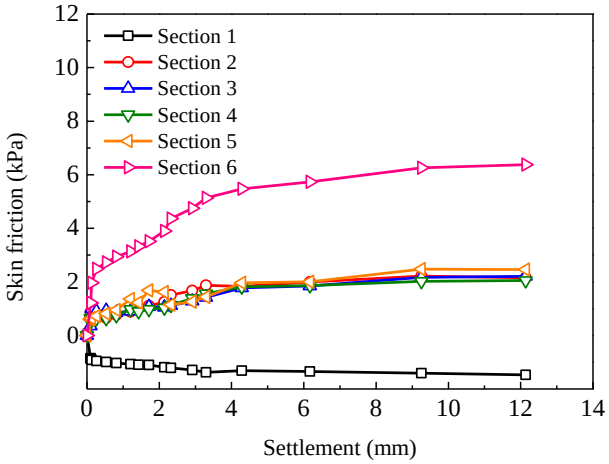

(b) Underlying layer: sandy soil

Fig. 16 Comparison curves of the distributions of skin friction under different loads

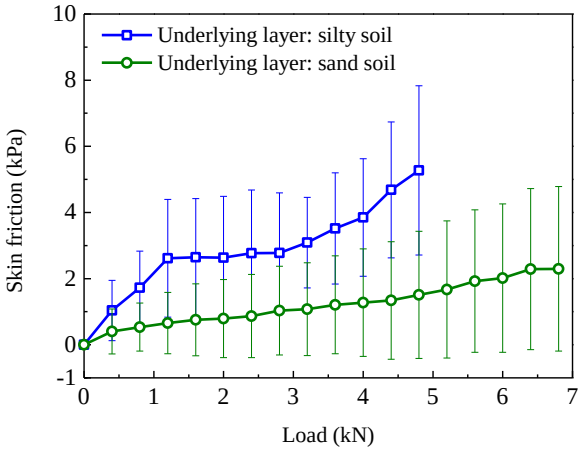

Fig. 17 Comparison of skin frictions under different loads

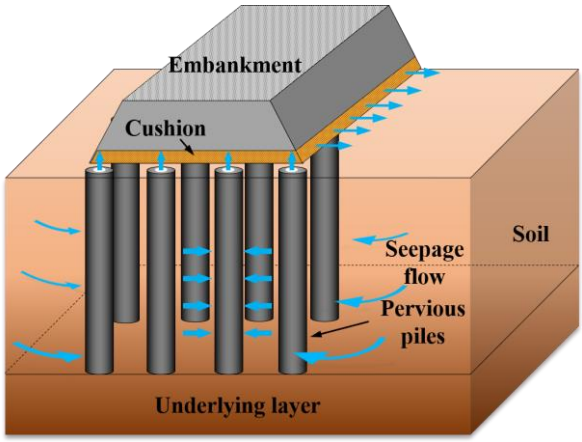

Fig. 18 Schematic of the application of the pervious concrete piles

layer; the greater the axial force (combined with Fig. 8) is, the greater the bearing capacity of the pile provided by the pile tip. For example, at a load of 4800 N, the skin friction is 1.51 kPa in the sandy underlying layer and 5.27 kPa in the silt layer. At this load, the skin friction of the silty underlying layer is 3.5 times that of the sand layer.

6. Discussions

6.1 Comparison of pervious and impervious concrete piles

The reinforcement mechanism of the pervious concrete pile foundation reinforcement technology has three advantages: first, the porous structure allows drainage through the piles; second, the rough surface provides more friction along the piles; and third, the use of high-strength ordinary Portland cement provides a pile bearing capacity sufficient to support the vertical load. These characteristics accelerate soil consolidation. As shown in Fig. 8, the pervious concrete piles have a high compressive strength; driving into the underlying layer can provide end resistance. Therefore, the bearing capacity of the soil near a pervious concrete pile is improved, and the stiffness of the pile can ensure its share of the upper load, so the bearing capacity of the composite foundation can be enhanced. Furthermore, a pile body is a continuous porous medium; the soil embedded in the pile body can provide frictional resistance for the composite foundation in the reinforcement process.

6.2 Comparison of different underlying layers

The penetration of a pile into a cushion or underlying layer to produce deformation is a necessary condition for the pile and soil to bear the load together. The vertical stress of a pervious concrete pile Q is

$$Q = Q_s + Q_p \tag{5}$$

where Q_s is the skin friction of the pervious concrete pile and Q_p is the end resistance of the pervious concrete pile.

The different responses of the settlement, pile–soil stress ratio, axial force, and skin friction in the different composite foundations reveal that the pervious concrete piles in these foundations perform differently. The bearing capacity of silt is lower than that of sand, and so the silty underlying layer cannot provide a sufficient bearing capacity at a high load level. Therefore, in the consolidation process, a pervious concrete pile settles with the soil, and pore water dissipates through the

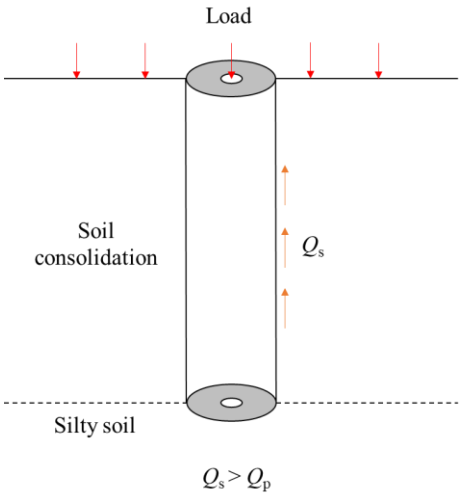

(a) Underlying layer: silty soil

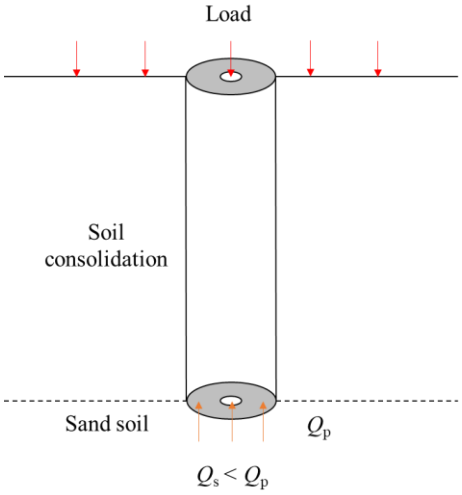

(b) Underlying layer: sandy soil

Fig. 19 The mechanical performance of pervious concrete piles in different underlying layers

pervious concrete pile; thus, the pile deformation cannot coordinate with the soil deformation, and the pervious concrete pile functions as a floating pile (Fig. 19(a)). However, regarding a sandy underlying layer, sandy soil can provide a greater bearing capacity than silty soil, the load is transferred from the pile to the sand layer, which bears the burden, and the pervious concrete pile acts as an end-bearing pile (Fig. 19(b)). Even though the mechanical performance of pervious concrete piles depends on the underlying layer, the same methods used for impervious concrete piles are used to improve the bearing capacity of pervious concrete piles.

7. Conclusions

The pervious concrete model piles were applied in silty and sandy underlying layers to investigate the bearing characteristics of the pervious concrete piles in composite foundations. As a result, the settlement, pile–soil stress ratio, and skin friction during multistage loading were obtained for comparison. The main conclusions were as follows:

- Pervious concrete piles with porous structures, rough surfaces and high-strength, they can provide the same strength and drainage path as impervious concrete piles while accelerating foundation consolidation and increasing the foundation bearing capacity.
- The bearing capacity of a silty underlying layer foundation is 33% lower than that with a sandy underlying layer foundation. However, with increasing soil layer thickness and pile length, the difference in the bearing capacities of pervious concrete piles in different underlying layers may decrease.
- The pile–soil stress ratio of the sandy underlying layer increases rapidly and decreases after it reaches the peak value of 27. On the other hand, the pile–soil stress ratio of the silty underlying layer increases gradually and decreases after it reaches the maximum value of 26. The maximum pile–soil stress ratios of the two foundation types are not different.
- The maximum axial force of a pervious pile in the sand can reach 4.7 kN, which is 1.8 kN greater than the ultimate force in the silt. Therefore, the skin friction of the pervious pile in silt is nearly 2 kN greater than that in sand. These results indicate that the pervious concrete pile in the sandy underlying layer can provide more axial force than that in the silty underlying layer, and the pervious concrete pile in the silty underlying layer can provide more skin friction than that in the sandy underlying layer.
- The performance of pervious concrete piles in the silty and sand underlying layer foundations varies, and these piles can reinforce foundations in different ways. In an underlying layer of silt, which has a bearing capacity lower than that of sand, the pile functions as a friction pile. In an underlying layer of sand, which has a bearing capacity higher than that of silt, the pile functions as an end-bearing pile.

Acknowledgments

The authors gratefully acknowledge the National Nature Science Foundation of China (Grant No. 41977241) and Changjiang Survey Planning Design and Research Co., Ltd Research Project (Grant No. CX2022Z34).

References

ACI (2006), "Pervious concrete", ACI 522R-06, American Concrete Institute, Farmington Hills, USA.

ACI (2010), "Report on pervious concrete", ACI 522R, American Concrete Institute, Farmington Hills, USA.

API (1987), "Recommended practice for planning, designing and constructing fixed offshore platforms: API recommended practice, 2A (RP 2A)", 17th Ed., Washington, DC: API.

Bahadori, H. and Farzalizadeh, R. (2018), "Dynamic properties of saturated sands mixed with tyre powders and tyre shreds", *Int. J Civil Eng.*, **16**(4), 395-408. https://doi.org/10.1007/s40999-016-0136-9.

Bahadori, H. and Manafi, S. (2015), "Effect of tyre chips on dynamic properties of saturated sands", *Int. J. Phys. Model. Geotech.*, **15**(3), 116-128. https://doi.org/10.1680/jphmg.13.00014.

Bahadori, H., Farzalizadeh R., Barghi, A. and Hasheminezhad, A.

(2018), "A comparative study between gravel and rubber drainage columns for mitigation of liquefaction hazards", *J. Rock Mech. Geotech. Eng.*, **10**(2018), 924-934. https://doi.org/10.1016/j.jrmge.2018.03.008.

CJJ/T 135-2009 (2009), "The technical specifications for pervious concrete pavement", Ministry of Housing and Urban-Rural Development of People's Republic of China.

Cui, X.Z., Jin, Q., Cui, S., Zhang, J. and Zhang, X. (2021), "Approximate experimental simulation of clogging of pervious concrete pile induced by soil liquefaction during earthquake", *J. Test Eval.*, **49**(1), 82-95. https://doi.org/10.1520/JTE20200048.

DB37/T 5124-2018 (2018), "Technical code for composite foundation of pervious pile", Housing and Urban-Rural Development Department of Shandong Province & Shandong administration of Market Regulation.

GB/T 50783-2012 (2012), "Technical code for composite foundation", Ministry of Housing and Urban-Rural Development of People's Republic of China, 2012.

Ghafoori, N. and Dutta, S. (1995), "Laboratory investigation of compacted no-fines concrete for paving materials", *J. Mater. Civil Eng.*, **7**(3), 183-191. https://doi.org/10.1061/(ASCE)0899-1561(1995)7:3(183).

Gong, J. and Qin, A. (2022), "Analytical solution for axisymmetric consolidation of unsaturated composite foundation incorporating permeable columns and impermeable columns", *Int. J. Numer. Anal. Method. Geomech.*. **47**, 609-626. https://doi.org10.1002/nag.3484.

Han, B. and Lu, M. (2023), "Theoretical study of consolidation of composite ground with permeable concrete piles considering pile penetration deformation", *Rock Soil Mech.*, **8**(44), 2360-2368. https://doi.org/10.16285/j.rsm.2022.1364.

Haselbach, L.M. and Freeman, R.M. (2007), "Effectively estimating in situ porosity of pervious concrete from cores", *J. ASTM Int.*, 4(7), 1-11. https://doi.org/10.1520/JAI100293.

Hasheminezhad, A. and Bahadori, H. (2019), "Seismic response of shallow foundations over liquefiable soils improved by deep soil mixing columns", *Comput. Geotech.*, **110**, 251-273. https://doi.org/10.1016/j.compgeo.2019.02.019.

Hasheminezhad, A. and Bahadori, H. (2020), "On the deep soil mixing method in the mitigation of liquefaction-induced bearing capacity degradation of shallow foundations", *Geomech. Geoeng.*, **17**(1), 334-346. https://doi.org/10.1080/17486025.2020.1755460.

Hsai-Yang, F. (1991), "Foundation engineering handbook", Springer, Boston, MA. https://doi.org/10.1007/978-1-4757-5271-7.

Huang, B., Wu, H. Shu, X. and Burdette, E.G. (2010), "Laboratory evaluation of permeability and strength of polymer-modified pervious concrete", *Constr. Build. Mater.*, **24**(5), 818-823. https://doi.org/10.1016/j.conbuildmat.2009.10.025.

Huang, Y., Wang, J. and Mei, G. (2016), "Model experimental study of accelerating dissipation of excess pore water pressure in soil around a permeable pipe pile", *Rock Soil Mech.*, **10**(37), 2893-2908. https://doi.org/10.16285/j.rsm.2016.10.021.

Kayhanian M., Anderson D., Harvey J.T., Jones, D. and Muhunthan, B. (2012), "Permeability measurement and scan imaging to assess clogging of pervious concrete pavements in parking lots", *J. Environ. Management*, **95**(1), 114-123. https://doi.org/10.1016/j.jenvman.2011.09.021.

Le, Y., Wang, N., Hu, W., Geng, D., Cai, Y. and Peng, Y. (2022), "Vertical dynamic impedance of a sand-filled nodular pile in saturated soil", *Ocean Eng.*, **259**, 112075. https://doi.org/10.1016/j.oceaneng.2022.112075.

Lin, H., Suleiman, M.T., Jabbour, H., Brown, D., and Kavazanjian, E., (2016), "Enhancing the axial compression response of pervious concrete ground improvement piles using biogrouting", *J. Geotech. Geoenviron. Eng.*, **142**(10), 04016045. https://doi.org/10.1061/(ASCE)GT.1943-5606.0001515.

Liu, P. and Yang, G. (2012), "Pile-soil self-balanced composite foundation design considering pile-end piercing settlement", *Rock Soil Mech.*, **33**(2), 539-546. https://doi.org/10.3969/j.issn.1000-7598.2012.02.034.

Malaiskiene, J. Kizinievic, O. and Sarkauskas, A. (2020), "The impact of coarse aggregate content on infiltration rate, structure and other physical & mechanical properties of pervious concrete", *Eur. J. Environ. Civil Eng.*, **24**(5), 569-582. https://doi.org/10.1080/19648189.2017.1410231.

Montes, F., Valavala, S. and Haselbach, L.M. (2005), "A new test method for porosity measurements of portland cement pervious concrete", *J. ASTM Int.*, **2**(1), 1-13.

Neithalath, N., Sumanasooriya, M.S. and Deo, O. (2010), "Characterizing pore volume, sizes, and connectivity in pervious concretes for permeability prediction", Mater. Characterization, **61**(8), 802-813. https://doi.org/10.1016/j.matchar.2010.05.004.

Neville, A.M. (1996), "Properties of concrete", Essex, England: Addison Wesley Longman Limited.

Ni, L., Suleiman, M.T. and Raich, A. (2016), "Behavior and soil-structure interaction of pervious concrete ground-improvement piles under lateral loading", *J. Geotech. Geoenviron. Eng.*, **142**(2), 4015071. https://doi.org/10.1061/(ASCE)GT.1943-5606.0001393.

Pan, H., Du, G., Xia, H., Wang, H. and Qin, D. (2021), "Quality assessment of dry soil mixing columns in soft soil areas of Eastern China", *Appl. Sci.*, **11**(21), 9957. https://doi.org/10.3390/app11219957.

Peng, Y., Ding, X., Yin, Z. and Wang, P. (2022), "Micromechanical analysis of the particle corner breakage effect on pile penetration resistance and formation of breakage zones in coral sand", *Ocean Eng.*, **259**, 111859. https://doi.org/10.1016/j.oceaneng.2022.111859.

Qi, C., Li, R., Gan, F., Zhang, W. and Han, H. (2020), "Measurement and simulation on consolidation behaviour of soft foundation improved with prefabricated vertical drains", *Int. J. Geosynth. Ground Eng.*, **6**, 23. https://doi.org/10.1007/s40891-020-00208-z..

Qin, Y.H., Liang, J., Yang, H. and Deng, Z. (2016), "Gas permeability of pervious concrete and its implications on the application of pervious pavements", *Measurement*, **78**, 104-110. https://doi.org/10.1016/j.measurement.2015.09.055.

Rashma, R.S.V., Jayalekshmi. B.R. and Shivashankar, R. (2021), "Shear strength behaviour of pervious concrete column improved soft clay bed: a numerical study", *Transport. Infrastruct. Geotechnol.*, **9**, 543-562. (Online). https://doi.org/10.1007/s40515-021-00179-2.

Schaefer, V.R. and Wang, K. (2006), "Mix design development for pervious concrete in cold weather climates", Iowa State University.

Suleiman, M.T., Ni, L. and Raich, A. (2014), "Development of pervious concrete pile ground-improvement alternative and behavior under vertical loading", *J. Geotech. Geoenviron. Eng.*, **140**(7), 4014035. https://doi.org/10.1061/(ASCE)GT.1943-5606.0001135.

Tamai, M., Kawai, A. and Kitada, H. (1992), "Properties of no-fines concrete in sea water and possibility of purifying water quality", *JCA Proceedings of Cement and Concrete*,. **46**, 880-885.

Teja, M., Mohammad, M.K. and Kalyan, K.G. (2020), "Axial and lateral loading behaviour of pervious concrete pile", *Indian Geotech. J.*, **50**(3), 505-513. https://doi.org/10.1007/s40098-019-00377-3.

Tennis, P.D., Leming, M.L. and Akers, D.J. (2004), "Pervious concrete pavements (No. PCA Serial No. 2828)", Portland Cement Association, Skokie, Illinois.

Wang, A., Zhang, Y., Xia, F., Luo, R. and Wang, N. (2022), "Study of

the lateral bearing capacity and optimization reinforcement scheme of an open caisson with consideration of soil disturbance", *Appl. Sci*., **12**(11), 5498. https://doi.org/10.3390/app12115498.

Wen, L., Kong, G., Li, Q. and Zhang, Z. (2020), "Field tests on axial behavior of grouted steel pipe micropiles in marine soft clay", *Int. J. Geomech*., **20**(6), 06020006. https://doi.org/10.1061/(ASCE)GM.1943-5622.0001656.

Wu, Y.D., Liu, J. and Chen, R. (2015), "An analytical analysis of a single axially-loaded pile using a nonlinear softening model", *Geomech. Eng*., **8**(6), 769-781. https://doi.org/10.12989/gae.2015.8.6.769

Yahia, A. and Kabagire, K.D. (2014), "New approach to proportion pervious concrete", *Constr. Build. Mater*., **62**, 38-46. https://doi.org/10.1016/j.conbuildmat.2014.03.025.

Yu, C., Zhang, A., Wang, Y. and Ren, W. (2020), "Analytical solution for consolidation of combined composite foundation reinforced with penetrated impermeable columns and partially penetrated permeable stone columns", *Comput. Geotech*., **124**(2020), 103606. https://doi.org/10.1016/j.compgeo.2020.103606.

Zhang, J., Cui, X.Z., Lan, R.Y., Zhao, Y.L., Lv, H.B., Xue, Q. and Chang, C.L. (2017), "Dynamic performance characteristics of pervious concrete pile composite foundations under earthquake loads", *J. Perform. Constr. Fac*., **31**(5), 04017064. https://doi.org/10.1061/(ASCE)CF.1943-5509.0001056.

CC